Tribology International 67 (2013) 72–80

Contents lists available at ScienceDirect

Tribology International

journal homepage: www.elsevier.com/locate/triboint

Torque loss in cylindrical roller thrust bearings lubricated with wind turbine gear oils at constant temperature

Carlos M.C.G. Fernandes [a,*], Pedro M.P. Amaro [b], Ramiro C. Martins [a], Jorge H.O. Seabra [b]

[a] INEGI, Universidade do Porto, Campus FEUP, Rua Dr. Roberto Frias 400, 4200-465 Porto, Portugal
[b] FEUP, Universidade do Porto, Rua Dr. Roberto Frias s/n, 4200-465 Porto, Portugal

ARTICLE INFO

Article history:
Received 8 January 2013
Received in revised form
3 June 2013
Accepted 27 June 2013
Available online 4 July 2013

Keywords:
Wind turbine gear oils
Rolling bearings
Friction torque
Efficiency

ABSTRACT

Six fully formulated wind turbine gear oils with the same viscosity grade and different formulations were selected and their physical properties were determined.

Cylindrical roller thrust bearing friction torque tests were performed on a modified Four-Ball Machine at a constant temperature of 80 °C under the following operating conditions: speed between 75 and 1200 rpm and two loads (700 N and 7000 N).

The experimental results showed that wind turbine gear oil formulation has a significant influence on rolling bearing friction torque.

1. Introduction

The generation of electricity by wind power is becoming more popular due to the concerns about the effects of global warming increase [1,2]. The levels of efficiency demanded in wind power generation mean that only one type is really suitable for use: planetary gearboxes [1]. In order to increase gearbox efficiency it is important to identify the main sources of power loss. The most common losses are friction loss between the meshing teeth [3–8], friction loss in the bearings [3,9,10], friction loss in the seals [3], lubricant churning losses [11,12] and energy loss due to air-drag [13].

Gearboxes have plagued the wind power industry [14–17]. Wind turbine gearbox problems start with the operating temperature of the oil. According to DIN recommendations the best viscosity and anti-scuffing properties are reached for oil operating temperatures above 80 °C. In wind turbine gearboxes that temperatures do not exceed 60 °C the anti-scuffing class tends to drop, resulting in a worst start-up behaviour and higher debris produced [18]. On the other hand, in order to assure an effective lubricant film the oil must be synthetic if the oil sump is higher than 80 °C due to the viscosity index [19,20]. Most wind turbine gearbox failures are rooted to the bearings [14–17]. The most significant fatigue wear phenomena are micropitting and smearing caused by large amounts of roller/raceway sliding in situations in which specific film thickness (Λ) is low, leading to high stresses and temperatures in the contact [21–24].

The internal friction torque generated inside rolling bearings has a significant contribution to machinery power loss, being essential to understand and measure it. A conventional four-ball machine (Cameron-Plint TE 82/7752) was adapted, in order to assemble a rolling bearing where the internal friction torque of cylindrical roller thrust bearings (RTB) can be measured under wide ranges of operating conditions (load, speed, temperature and lubricant) [25].

In previous works [26,27], the friction torque generated in cylindrical roller thrust bearings and thrust ball bearings lubricated with wind turbine gear oils was measured in auto-induced temperature conditions. In the present work the operating temperature was kept constant in order to maintain the same viscosity characteristics of the lubricants for different speeds and loads. For that purpose, rolling bearing tests were performed, using cylindrical roller thrust bearings (RTB - 81107) lubricated with wind turbine gear oils (ISOVG 320) at constant temperature, during which the internal friction torque was measured for low and high load, 700 and 7000 N, respectively, and varying the rotational speed between 75 and 1200 rpm. The low load applied is still higher than the minimum load required by the bearing. Previously the same was done for a thrust ball bearing [28]. The results obtained aim to clarify the influence of gear oil formulation on rolling bearing friction torque for different loads and speeds.

2. Lubricant properties

The six fully formulated gear oils have a viscosity grade ISO VG 320. The formulations are the following: ESTF and ESTR are biodegradable ester base oils; MINR is a mineral base oil; MINE

* Corresponding author. Tel.: +351 225082212.
E-mail address: cfernandes@inegi.up.pt (C.M.C.G. Fernandes).

0301-679X/$ - see front matter © 2013 Elsevier Ltd. All rights reserved.
http://dx.doi.org/10.1016/j.triboint.2013.06.016

Table 1
Physical and chemical properties of wind turbine gear oils used.

Parameter	Unit	MINR	ESTR	PAOR	ESTF	MINE	PAGD
Base oil	(/)	Mineral	Ester	Polialphaolefin	Ester	Mineral + PAMA	Polyalkyleneglycol
Chemical composition							
Zinc (Zn)	(ppm)	0.9	6.6	3.5	0.7	< 1	1
Magnesium (Mg)	(ppm)	0.9	1.3	0.5	1.3	< 1	1.4
Phosphorus (P)	(ppm)	354.3	226.2	415.9	449.4	460	1100
Calcium (Ca)	(ppm)	2.5	14.4	0.5	n.d.	2	0.8
Boron (B)	(ppm)	22.3	1.7	28.4	33.6	36	1.0
Sulphur (S)	(ppm)	11200	406	5020	5030	6750	362
Physical properties							
Density at 15 °C	(g/cm^3)	0.902	0.915	0.859	0.957	0.893	1.059
Thermal expansion coefficient ($\alpha_t \times 10^{-4}$)	(/)	−5.8	−8.1	−5.5	−6.7	−6.7	−7.1
Viscosity at 40 °C	(cSt)	319.22	301.93	313.52	323.95	328.30	289.13
Viscosity at 70 °C	(cSt)	65.81	79.84	85.41	88.98	93.19	104.52
Viscosity at 100 °C	(cSt)	22.33	30.71	33.33	34.84	37.13	48.09
m	(/)	9.066	7.582	7.351	7.261	7.048	5.759
n	(/)	3.473	2.880	2.787	2.749	2.663	2.151
Thermoviscosity at 40 °C ($\beta \times 10^{-3}$)	($°K^{-1}$)	63.88	49.09	50.68	49.90	49.33	37.34
Thermoviscosity at 70 °C ($\beta \times 10^{-3}$)	($°K^{-1}$)	42.83	35.25	36.16	35.78	35.48	28.36
Thermoviscosity at 100 °C ($\beta \times 10^{-3}$)	($°K^{-1}$)	30.07	26.19	26.72	26.55	26.40	22.12
s at 0.2 GPa	(/)	0.9904	0.6605	0.7382	0.6605	0.7382	0.5489
t at 0.2 GPa	(/)	0.1390	0.1360	0.1335	0.1360	0.1335	0.1485
Piezoviscosity at 40 °C ($\alpha \times 10^{-8}$)	(Pa^{-1})	2.207	1.437	1.590	1.450	1.600	1.278
Piezoviscosity at 70 °C ($\alpha \times 10^{-8}$)	(Pa^{-1})	1.774	1.212	1.339	1.220	1.353	1.105
Piezoviscosity at 100 °C ($\alpha \times 10^{-8}$)	(Pa^{-1})	1.527	1.071	1.182	1.076	1.197	0.988
VI	(/)	85	140	150	153	163	230

is formulated with hydroprocessed group III base oil and a PAMA thickener; PAGD is a polyalkylene glycol and PAOR is a polyalphaolefin base oil with an ester compatibilizer. Table 1 displays the wind turbine gear oils physical properties as well as their chemical composition.

2.1. Chemical composition

Using the ICP method according to ASTM:D 5185, the chemical composition of the lubricants was determined and presented in Table 1. The elements identified were Zinc (Zn), Magnesium (Mg), Phosphorus (Ph), Calcium (Ca), Boron (B) and Sulphur (S). It is clear that the formulations are significantly different, both in terms of base oil and additive package.

2.2. Physical properties

A complete characterization of physical properties of the lubricants was performed. A detailed description of the physical properties are presented in Appendix A and the results are presented in Table 1.

3. Rolling bearing assembly and test procedures

The rolling bearing tests were performed on a modified Four-Ball machine, where the Four-Ball arrangement was replaced by a rolling bearing assembly, as shown in Fig. 1. This assembly was developed to test several rolling bearings and measure the friction torque as well as the operating temperature in several different points. A detailed presentation of this assembly can be found in [25].

The rolling bearing assembly is divided in two parts: the shaft adapter (6), directly connected to the machine shaft and supporting the bearing upper race (5); a lower race support (2) and the bearing lower race (3), both clamped to the bearing housing (1). In operation, the internal bearing torque (or friction torque) is transmitted to the torque cell (11) through the bearing housing (1). The friction torque was measured with a piezoelectric torque cell *KISTLER*9339 *A*, ensuring high-accuracy measurements even when the friction torque generated in the bearing was very small compared to the measurement range available.

This assembly includes five thermocouples (I–V), measuring temperatures at strategic locations (see Fig. 1) which are used to monitor the temperature inside the bearing assembly (IV), near to the rolling bearing and the lubricant (III) and to evaluate the heat evacuation from the bearing housing into the surrounding environment (I, II and V). The system is also monitored by two thermocouples to monitor the chamber and room temperatures.

For the axial loads applied (700 and 7000 N) each contact element (roller) reach the conditions presented in Table 2.

When assembled in the modified Four-Ball machine the rolling bearing assembly is submitted to a continuous air flow, forced by two 38 mm diameter fans running at 2000 rpm, cooling the chamber surrounding the bearing house.

The rolling bearing is lubricated by an oil volume of 14 ml. This volume was selected so that the oil level reaches the centre of the roller, such as advised by the manufacturer.

The rotational speeds were chosen considering the available range of our machine and also the rotational speeds usually used in the wind turbines. For example, the low speed planetary shaft is about 1 m/s and the high speed shaft is about 6.5 m/s.

The heater (Fig. 2) is used to increase and maintain a constant operating temperature at a desired value (80 °C for the study case). The thermocouple (III) is used to control the oil operating temperature, because the heater control system is a PID with feedback.

3.1. Total friction torque procedure

A detailed presentation of the test procedure can be found in [25].

The machine was started at the desirable speed and ran until it reached a constant operating temperature (80 °C), induced by the heaters. Under these conditions, four friction torque measurements were performed: three values are stored and the most dispersed one was disregarded. Due to the “drift effect”, which affects the measurements of the piezoelectric sensors after long periods of operation, the friction torque measurements should be made in a short period of

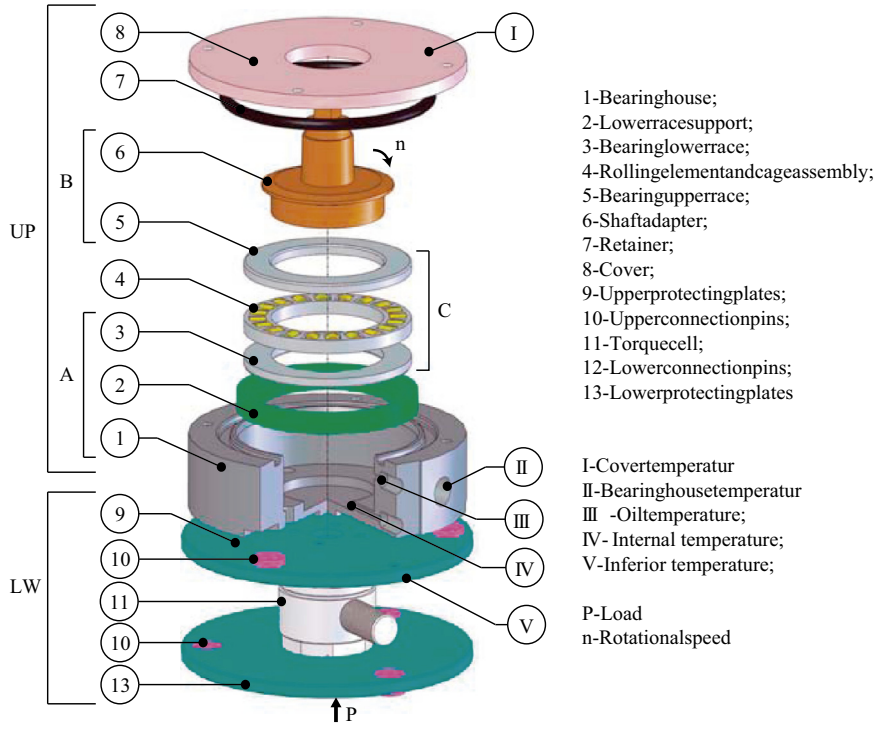

Fig. 1. Schematic view of the rolling bearing assembly.

Table 2
Roller-raceway contact parameters.

Axial load (N)	700	7000
R_X (m)	5.00×10^{-3}	
L (mm)	5.00	
a_h (μm)	13.76	43.50
p_0 (MPa)	318	1004

Table 3
Kinematic viscosity and piezo-viscosity at 80 °C.

Base oil	ESTF	ESTR	MINE	MINR	PAGD	PAOR
Kinematic viscosity (mm^2/s)	63.0	56.1	66.5	43.9	78.9	60.4
Piezoviscosity ($\alpha \times 10^{-8}$)	1.16	1.14	1.29	1.68	1.05	1.28

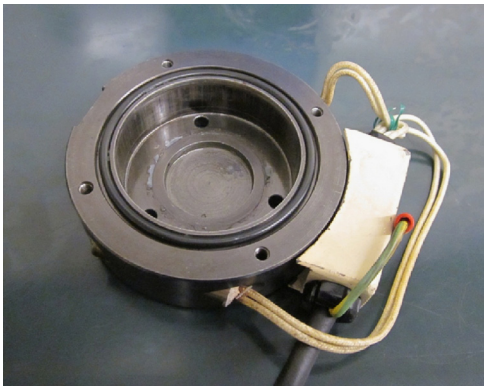

Fig. 2. Bearing house with heaters.

time (less than 120 s) and at constant temperature (80 °C). The measurements were taken after a 30 min time operation at the desirable speed, load and controlled temperature.

4. Results

4.1. Operating and stabilization temperature

The operating temperature was controlled with a PID control system that assures a temperature of 80 ± 0.5 °C. At 1200 rpm and 7000 N, the temperature reach higher values than the expected for some oils.

The stabilization temperatures of the RTB, defined as the difference between the operating and chamber temperatures, that is, $\theta_s = \theta - \theta_c$ are very similar for every test performed. The stabilization temperature of the RTB decreased when the operating speed increased. This variation is very small (≈2 °C) and occurs due to increasing the room temperature according with the daytime and consequently the chamber temperature increases.

4.2. Operating kinematic viscosity

The tests were performed at 80 °C, so the kinematic viscosity is the same for each oil and for all speeds and loads. In Table 3 the kinematic viscosity of each oil as well as its piezo-viscosity (α) are presented.

5. Film thickness in the roller-raceway contact

The centre film thickness in the roller-raceway contact of the RTB was determined using Dowson and Higginson [29] equation for linear contacts, as presented in Appendix B.

Another way to define the degree of separation between the surfaces is proposed by SKF [10], as shown in the following equation:

$$\kappa = \frac{\nu}{\nu_1} \tag{1}$$

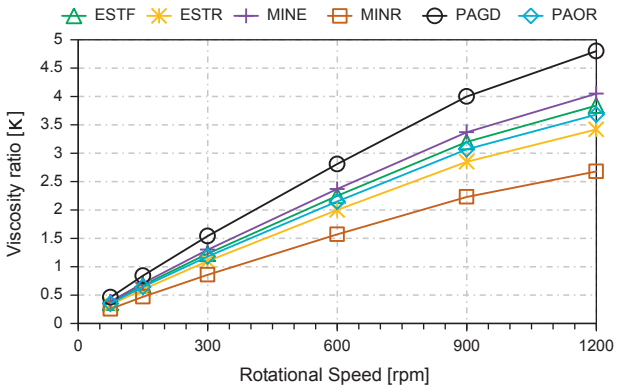

Fig. 3. Viscosity ratio vs rotational speed.

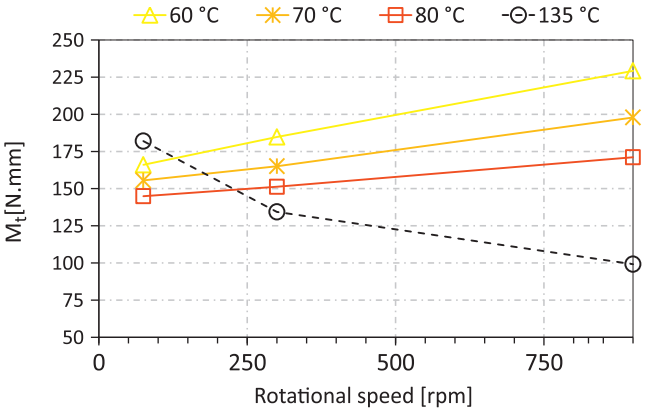

Fig. 4. Tests performed with PAOR to calibrate the model.

Since the viscosity ratio does not account for the load, Fig. 3 presents the viscosity ratio for the speeds tested in this work, at 700 and 7000 N. For $\kappa > 2$ the contact lies in full film conditions.

6. Friction torque model

In order to understand the friction torque behaviour of the rolling bearings lubricated with each wind turbine gear oil, the model proposed by SKF [10] was used (see Appendix C).

The numeric model proposed by SKF [10] was applied on the experimental results. Even though the model was able to characterize the rolling bearings friction torque in previous works [26,27], in the present work the operating temperature is much higher than the temperature obtained in a self induced situation, resulting in a much lower operating kinematic viscosity and in worse correlations in the model results. This occurs probably due to the inefficient identification of the real lubrication regime occurring in the tests performed. The model suggests that for low speed, the viscosity of the lubricant is not able to separate the surfaces, and addresses a boundary film lubrication for the lower speeds tested 75–150 rpm.

In order to calibrate the model a matrix of 3 speeds and 3 temperatures test points was obtained, using the PAOR lubricant and a thrust ball bearing, see [28].

In this test the main objective was to identify the lubrication regime of the tests performed. With this test the influence of the speed and temperature in the total friction torque generated within the rolling bearing was characterized. After these tests the influence of the temperature indicated that the increase of temperature caused a decrease of the friction torque (60 °C, 70 °C and 80 °C). The Stribeck curve suggests that this phenomena occurs when the test is performed in full film conditions. To consider the idea that the tests performed at 80 °C are in full film conditions we increased the temperature (decreases the viscosity) of the test in order to decrease the film thickness and in this way promote higher friction torque. See in Fig. 4 the line corresponding to 135 °C. For 75 rpm the friction torque increased substantially, giving the idea that the test tends towards a mixed or boundary film lubrication.

In Fig. 4 measurements of the friction torque in four different temperatures and three different speeds for a thrust ball bearing are presented. The calibration procedure was made for a thrust ball bearing as well as for a roller thrust bearing. But, in fact, the test condition at 135 °C was not possible to realize with a roller thrust bearing due to the polyamide cage that was not suitable to perform higher than 110 °C. The behaviour verified with a roller thrust bearing was the same of a thrust ball bearing when temperature is changed between 60, 70 and 80 °C, so that a higher temperature generate lower friction torque.

Considering the possibility that the tests are performed under full film conditions, the numeric model was modified in order to fill this disagreement observed on the sliding friction torque weighting factor (ϕ_{bl}) that depends essentially on the lubrication regime. Initially the model suggests that for lower speed the test performed in boundary regime, because $\phi_{bl} \approx 1$. The ϕ_{bl} parameter was determined by Eq. (2). In order to modify the parameter influence in the lubrication regime quantification, the exponent 1.4 was replaced by 1.8 (see Eq. (3)), considering the results mentioned above.

$$\phi_{bl} = \frac{1}{e^{2.6\times10^{-8}(n.\nu)^{1.4}d_m}} \tag{2}$$

$$\phi_{bl-modified} = \frac{1}{e^{2.6\times10^{-8}(n.\nu)^{1.8}d_m}} \tag{3}$$

7. Results and discussion

The SKF friction torque model was used to predict the values of the rolling (M_{rr}) and sliding (M_{sl}) friction torques, and of the EHD (μ_{EHD}) and sliding (μ_{sl}) coefficients of friction for all testing conditions considered in the cylindrical roller thrust bearing tests under an axial load of 700 N and 7000 N, respectively, 2.4% and 24% of dynamic load capacity of the RTB. The corresponding specific lubricant film thickness was also estimated. For the oils MINE, MINR, PAGD and PAOR, tested at 1200 rpm under 7000 N load, it was not possible to keep the operating temperature at 80 °C and the RTB reached higher operating temperatures.

7.1. Axial load 7000 N

Fig. 5a shows that when the operating speed increases from 75 rpm to 1200 rpm the specific lubricant film thickness inside the RTB increased from 0.2 to 1.10/1.80 depending on the oil tested, meaning that the lubrication regime evolved from boundary to mixed film lubrication. All gear oils exhibited a similar trend, but PAGD oil showed significant higher values of Λ due to its higher viscosity at 80 °C.

Fig. 5c shows the rolling torque estimated for the RTB in all operating conditions. As expected, and because the tests were performed at constant temperature (80 °C), when the speed increases the rolling torque also increases ($M_{rr} \propto (n.\nu)^{0.6}$). This figure also shows that oils ESTF, ESTR, MINE and PAOR generated very similar rolling torques, because they have the same viscosity grade (ISO VG 320) and similar viscosities at 80 °C. PAGD oil produces

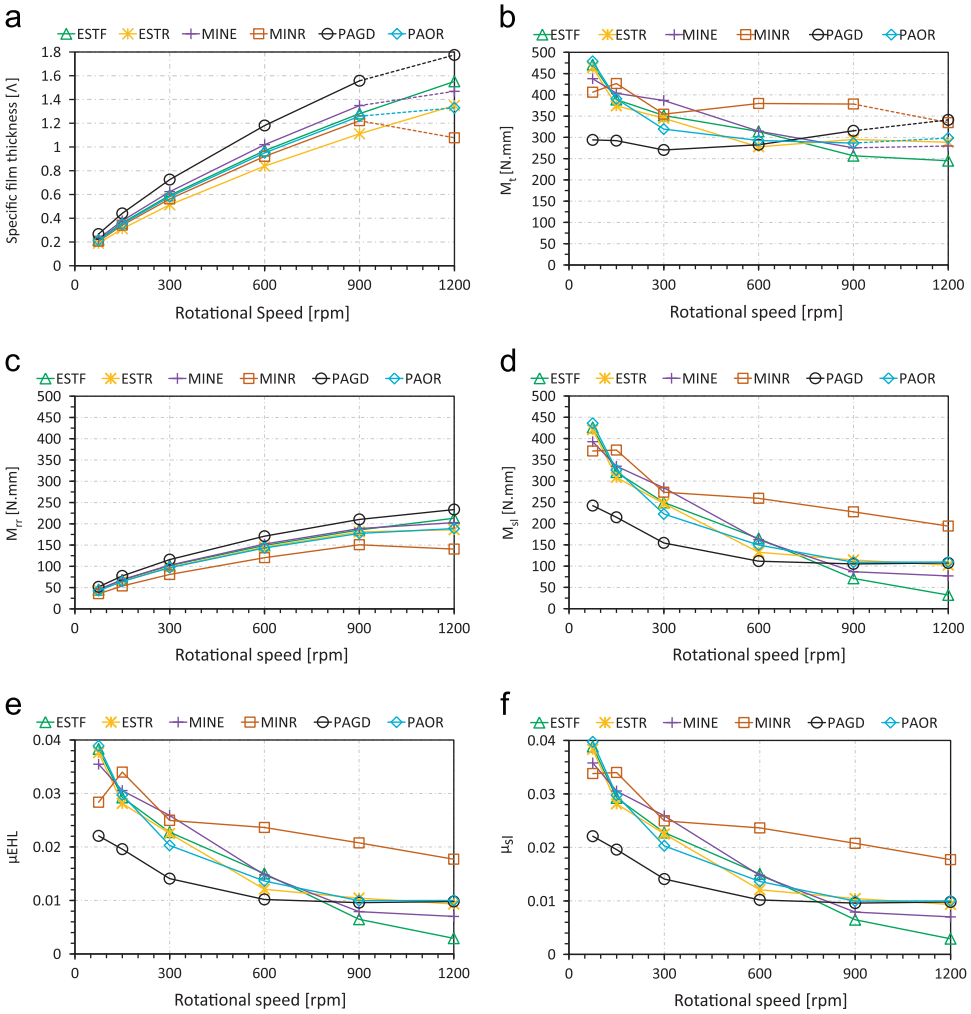

Fig. 5. Λ, M_t, M_{rr}, M_{sl}, μ_{EHL} and μsl for RTB – axial load 7000 N. (a) Specific film thickness. (b) Total friction torque. (c) Rolling friction torque. (d) Sliding friction torque. (e) μ_{EHL} friction coefficient. (f) Sliding friction coefficient.

very high rolling torques because it has the highest VI and the highest viscosity at 80 °C, while MINR oil, on the other hand it has the lowest VI and the lowest viscosity at 80 °C.

Fig. 5d shows the sliding torque estimated for the RTB in all operating speed conditions. The sliding torque is obtained by subtracting the rolling friction torque to the experimental friction torque, that is, $M_{sl} = M_{exp} - \phi_{ish}.\phi_{rs}.M_{rr}$. The experimental friction torque ($M_{exp} = M_t$, see Fig. 5b) decreased when speed increased, the opposite trend of the rolling torque, consequently the sliding torque decreases, as shown in Fig. 5d. Such behaviour is typical of RTB operating under the mixed film lubrication regime and the sliding coefficient of friction μ_{sl} decreased significantly when speed increased, at constant temperature, as presented in Fig. 5d.

Comparing the sliding coefficient of friction (μ_{sl}) with the full film coefficient of friction (μ_{EHL}) Fig. 5e and f, no significant differences are observed. Only at the lowest speed (75 rpm), at the smallest specific lubricant film thickness ($0.20 \leq \Lambda \leq 0.25$), $\mu_{sl} > \mu_{EHL}$.

Comparing the friction behaviour of the wind turbine gear oils, inside the cylindrical roller thrust bearings, it is very clear that MINR oil always produced the highest values of the sliding coefficient of friction, of the sliding torque and of the total rolling bearing friction torque, while PAGD oil always generated the lowest corresponding values. Oils ESTF, ESTR and PAOR were placed in between the previous two. However, at low speed the oils ESTF, ESTR and PAOR generated the highest sliding coefficient of friction, sliding torque and total friction torque.

7.2. Axial load 700 N

Fig. 6a shows that when the operating speed increases from 75 rpm to 1200 rpm the specific lubricant film thickness inside the RTB increases from 0.25 to 1.79/2.32, depending on the oil tested, meaning that the lubrication regime evolved from boundary to near full film lubrication. All gear oils exhibited a similar trend, but PAGD oil produced the highest Λ s, because of its high viscosity at 80 °C, and ESTR oil generated the lowest Λ s.

Fig. 6c shows the rolling torque estimated for the RTB in all operating conditions. As expected, and because the tests were performed at constant temperature (80 °C), when the speed increases the rolling torque also increases ($M_{rr} \propto (n.\nu)^{0.6}$). This figure also shows that the oils ESTF, ESTR, MINE and PAOR generated very similar rolling torques, because they have the same viscosity grade (ISO VG 320) and similar viscosities at 80 °C. PAGD oil produces very high rolling torques because it has the highest viscosity at 80 °C, while MINR oil, on the other hand, has the lowest viscosity at 80 °C.

The experimental friction torque ($M_{exp} = M_t$, see Fig. 6b) as well as the rolling torque (M_{rr}, see Fig. 6c) increases when speed increases, but at different rates. The sliding torque, obtained by

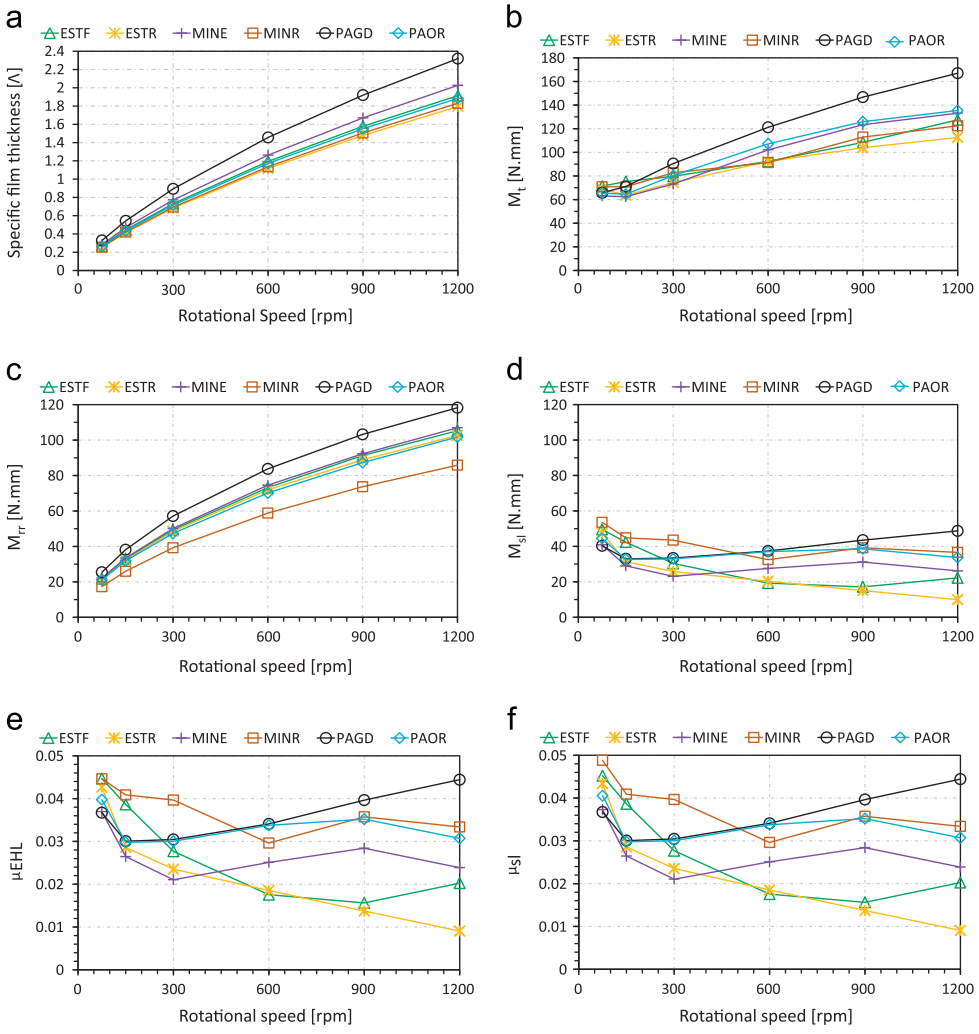

Fig. 6. Λ, M_t, M_{rr}, M_{sl}, μ_{EHL} and μsl for RTB – axial load 700 N. (a) Specific film thickness. (b) Total friction torque. (c) Rolling friction torque. (d) Sliding friction torque. (e) μ_{EHL} friction coefficient. (f) Sliding friction coefficient.

subtracting the rolling friction torque to the experimental friction torque, that is, $M_{sl} = M_{exp} - \phi_{ish}.\phi_{rs}.M_{rr}$ (see Fig. 6d), shows that the sliding torque has small variations with the speed for all operating conditions.

Comparing the friction behaviour of the wind turbine gear oils, inside the RTB, it is clear that PAGD oil always generated the highest total friction torque while the other produced similar total friction torque.

7.3. 7000 N vs 700 N

The rolling torque is influenced by the load in the following way, when the load is multiplied by 10 (from 700 to 7000 N) the rolling torque increases about 2 times for each speed. In the other hand, the sliding torque factor G_{sl} increases with proportionally with the load. The load increment results in higher total friction torque within the rolling bearing that increases with the speed.

The amount of the sliding torque in the total friction torque decreases when the speed increases for both loads applied. But its contribution is higher for the 700 N axial load.

8. Conclusion

The results achieved with the torque tests for roller thrust bearings, showed that

- The total friction torque, with an axial load of 7000 N, decreased when the operating speed increased, although this behaviour is not observed for an axial load of 700 N.
- For the friction torque components, the rolling torque increased with the increase of speed and the sliding torque decreased with the increase of speed, no matter what the applied load was.
- The coefficients of friction with an axial load of 7000 N had a clear decrease when the speed increased but, in the case of a load of 700 N there was not a clear trend when the speed increased.
- For the RTB loaded with 7000 N, at 1200 rpm, the operating temperature of some oils increased to values outside those expected for the experiments.
- For low load the following situation occurs: higher viscosity promotes higher torque loss. For high load higher torque loss is generated by oils with low viscosity index.
- The PAGD oil can promote a reduction higher than 25% of the power loss generated for high load and low speed.

Acknowledgments

The authors acknowledge to “Fundação para a Ciência e Tecnologia” for the financial support given through the project

"High efficiency lubricants and gears for windmill planetary gearboxes", with research contract PTDC/EME-PME/100808/2008.

Appendix A. Physical properties

A.1. Density

The densities of the gear oils at 15 °C are presented in Table 1. The gear oil densities were measured at 40, 70 and 100 °C using a *DMA*35 N densimeter. The values measured were used to calculate the thermal expansion coefficient α_t of the gear oils, according to Eq. (A.1). The results are presented in Table 1.

$$\rho = \rho_0 + \alpha_t.\rho_0(T - T_{ref}) \tag{A.1}$$

A.2. Kinematic viscosity

The kinematic viscosities of each oil were measured using an Engler viscometer. The measurements were performed at 40, 70 and 100 °C according to ASTM: D341 and are displayed in Table 1. At 40 °C all the kinematic viscosities were very similar, since all the gear oils had the same viscosity grade. However, at 100 °C the kinematic viscosities were significantly different: 22.3 cSt for the MINR oil, 51.6 cSt for the PAGD and 33.3, 34.9 and 36.6 for the PAOR, ESTR and ESTF, respectively.

The kinematic viscosities were used to determine the Viscosity Index of each lubricant. The MINR gear oil had the lowest VI (85) while the PAGD oil had the highest value (241). The PAOR, ESTR, ESTF gear oils had intermediate values, respectively, 153, 162 and 159.

A.3. Dynamic viscosity

The dynamic viscosities of the oils were also measured using a Contraves Rheomat 115 rheometer with a rotary viscometer with coaxial cylinders. The measurements were performed at 40, 70 and 100 °C, and several shear strain rates (6.387, 26.786, 112.477, 472.479 and 967.280). The results are displayed in Fig. A1. The corresponding kinematic viscosities are presented in Fig. A2.

At 40 °C the dynamic viscosity was not independent of the shear strain rate, indicating that the lubricant behaviour was non-Newtonian. At higher temperatures (70 and 100 °C) such non-Newtonian behaviour was no longer observed and the dynamic viscosity was constant whatever the shear strain rate. This behaviour was observed for all the gear oils.

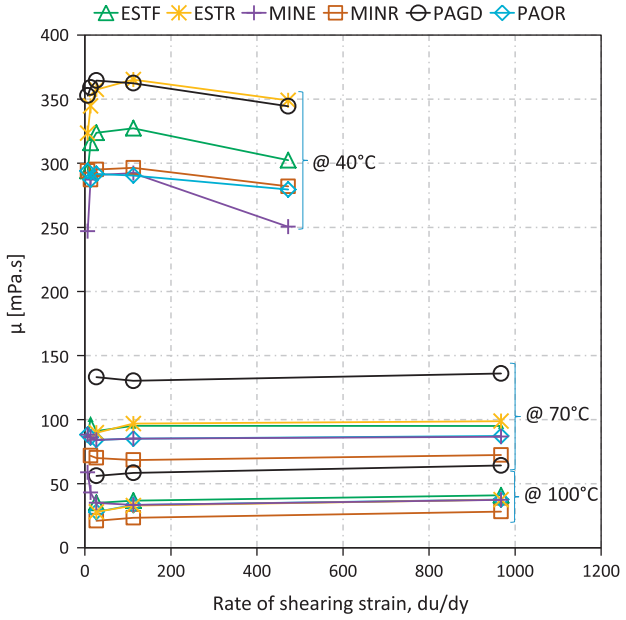

Fig. A1. Dynamic viscosity vs. shearing strain rate.

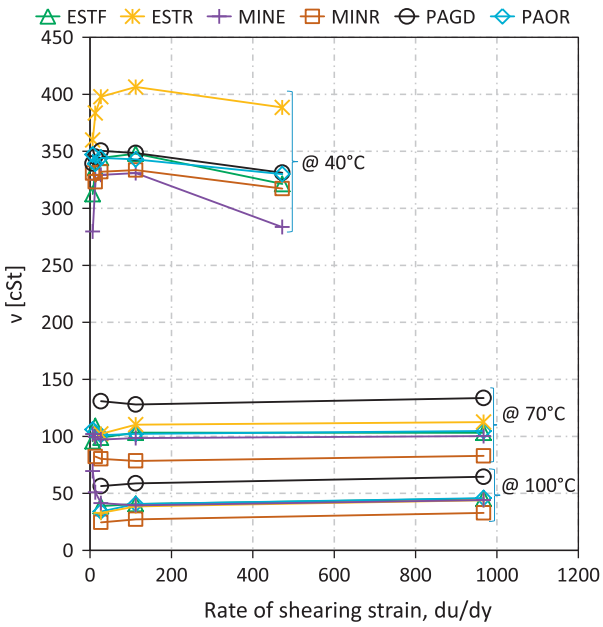

Fig. A2. Kinematic viscosity vs. shear strain rate.

A.4. Thermoviscosity

The kinematic viscosities were used to determine the thermo-viscosity of the oils, using the following equation:

$$\beta = \frac{m}{T}.\frac{(\nu + a).\ln(\nu + a)}{\nu} \tag{A.2}$$

The constants m and n (ASTM: D341) as well as the thermo-viscosity values calculated for each oil are presented in Table 1. The constant a is 0.7 according the standard. The thermoviscosity values follow the inverse trend of the Viscosity Index (high Viscosity Index imply a low thermoviscosity value).

A.5. Piezoviscosity

Gold et al. [30] proposed Eq. (A.3) to calculate the piezo-viscosity of oils formulated with different base oils

$$\alpha = s\nu^t \tag{A.3}$$

The piezoviscosity has a very significant influence on lubricant film thickness between roller and raceways in a roller thrust bearing.

Appendix B. Equations for the film thickness in the roller-raceway contact

The centre film thickness in the roller-raceway contact of the RTB can be determined using Eqs. (B.1)–(B.4) for linear contacts, derived by Higginson and Dowson [29],

$$h_0 = 0.975.R_X.U^{0.727}.G^{0.727}.W^{-0.091} \tag{B.1}$$

$$U = \frac{\eta_0.(U_1 + U_2)}{2.R_X.E^*} \tag{B.2}$$

$$G = 2.\alpha.E^* \tag{B.3}$$

$$W = \frac{F_n}{R_X.l.E^*} \tag{B.4}$$

The geometry of the roller-raceway contact in the RTB was used as well as the oil properties at the corresponding operating temperatures, in this case 80 °C.

The theoretical film thickness h_0 was corrected using the thermal reduction factor (ϕ_T) due to inlet shear heating, as shown in Eqs. (B.5)–(B.9). The specific film thickness was computed with Eq. (B.9), taking into account the composite roughness of the cylindrical roller thrust bearing ($\sigma = 0.14$ μm). Several measurements of the rollers and raceways surface roughness were made with an absolute stylus probe (measuring length 4.8 mm, cut-off 0.8 mm).

Knowing the specific film thickness in the roller-raceway contact, it is possible to evaluate the corresponding lubrication regimes.

$$h_{0C} = \phi_T.h_0 \tag{B.5}$$

$$\phi_T = \left\{1 + 0.1.(1 + 14.8S^{0.83}).L^{0.64}\right\}^{-1} \tag{B.6}$$

$$L = \frac{\beta.\eta_0.(U_1 + U_2)^2)}{K} \tag{B.7}$$

$$S = \frac{|U_1 - U_2|}{U_1 + U_2} \tag{B.8}$$

$$\Lambda = \frac{h_{0C}}{\sqrt{\sigma_1^2 + \sigma_2^2}} \tag{B.9}$$

Appendix C. Rolling bearing friction torque model

The friction torque model proposed by SKF [10] considers that the total friction torque is the sum of four different physical sources of torque loss, represented by the following equation:

$$M_t = M'_{rr} + M_{sl} + M_{drag} + M_{seal} \tag{C.1}$$

The cylindrical roller thrust bearing (81107) do not have seals so the M_{seal} torque loss term was disregarded. The drag losses were very small because the operating speeds and the mean diameter of the RTB are small and, consequently, the drag torque loss term was also disregarded. Thus, the total friction torques of the RTB had only two terms: the rolling and sliding torques, respectively, $M_{rr'}$ and M_{sl}, as represented in Eq. (C.1),

$$M_{exp} = M_t = M'_{rr} + M_{sl} \tag{C.2}$$

Since the total friction torque was measured experimentally ($M_t = M_{exp}$), it was possible to calculate the sliding torque once the rolling torque was known, see the following equation:

$$M_{sl} = M_t - M'_{rr} = M_{exp} - M'_{rr} \tag{C.3}$$

Eqs. (C.4)–(C.11) define the rolling and sliding torques

$$M_{rr'} = \phi_{ish}.\phi_{rs}[G_{rr}(n.\nu)^{0,6}] \tag{C.4}$$

Table C1
SKF rolling bearing constants.

	Cylindrical roller thrust bearing (81107)
S_1	0.154
R_1	2.25×10^{-6}
K_Z	4.4
K_L	0.43

$$\phi_{ish} = \frac{1}{1 + 1.84 \times 10^{-9}(nd_m)^{1.28}\nu^{0.64}} \tag{C.5}$$

$$\phi_{rs} = \frac{1}{e^{K_{rs}\nu n(d+D)\sqrt{\frac{K_Z}{2(D-d)}}}} \tag{C.6}$$

$$G_{rr} = R_1.d_m^{2,38}.F_a^{0,31} \tag{C.7}$$

$$M_{sl} = G_{sl}.\mu_{sl} \tag{C.8}$$

$$G_{sl} = S_1.d_m^{0,62}.F_a \tag{C.9}$$

$$\mu_{sl} = \phi_{bl}.\mu_{bl} + (1 - \phi_{bl}).\mu_{EHD} \tag{C.10}$$

$$\phi_{bl} = \frac{1}{e^{2,6\times10^{-8}(n.\nu)^{1.4}d_m}} \tag{C.11}$$

The constants S_1, R_1 and K_Z are given in Table C1.

The rolling torque (C.4) is mainly influenced by the viscosity of the gear oil, at the operating temperature, and by the rotational speed ($(n.\nu)^{0.6}$). The product of the "kinematic replenishment factor" by the "inlet shear heating factor" ($\phi_{rs}.\phi_{ish}$), decreases when the operating speed increases.

The sliding torque (C.3) is highly affected by the load weighting factor and by the coefficient of friction in full film EHD lubrication, ϕ_{bl} and μ_{EHD}, respectively. The load weighting factor ϕ_{bl} increases when the specific film thickness decreases and this affects the sliding coefficient of friction, μ_{sl}, and the sliding torque.

Notation and units

a	ASTM: D341 reference kinematic viscosity (cSt)
a_H	Hertz contact half width (μm)
C_0	ellipticity parameter (/)
d_m	rolling bearing mean diameter (mm)
E^*	contact equivalent Young modulus (Pa)
Fa	axial load (N)
G	material parameter (/)
G_{rr}	factor depending on the bearing type, bearing mean diameter and applied load (/)
G_{sl}	factor depending on the bearing type, bearing mean diameter and applied load (N mm)
h_0	centre film thickness (μm)
h_{0C}	thermal corrected centre film thickness (μm)
K_{rs}	starvation constant for oil bath lubrication (/)
K_Z	bearing type related geometry constant (/)
L	thermal parameter (/)
m	ASTM: D341 viscosity parameter (/)
M_{exp}	bearing friction torque measured experimentally (N mm)
M'_{rr}	rolling friction torque (N mm)
M_{sl}	sliding friction torque (N mm)
M_{drag}	friction torque of drag losses (N mm)
M_{seal}	friction torque of seals (N mm)
M_t	internal bearing friction torque (N mm)
n	ASTM: D341 viscosity parameter (/)
n	rotational speed (rpm)
R_1	geometry constant for rolling friction torque (/)
R_X	radius of curvature in x direction (/)
R_Y	radius of curvature in y direction (/)
S_1	geometry constant for sliding friction torque (/)
s	piezoviscosity parameter (/)
S	sliding factor of the roller/ball (/)
t	piezoviscosity parameter (/)
T	operating temperature (K)
T_{ref}	reference temperature (K)
U	speed influence parameter (/)

U_1	linear speed of roller (m/s)
U_2	linear speed of ring (m/s)
VI	viscosity index (/)
W	load parameter (/)
α	piezoviscosity coefficient (Pa^{-1})
α_t	thermal expansion coefficient (/)
β	thermoviscosity coefficient ($^{\circ}K^{-1}$)
η	dynamic viscosity (Pa.s)
ϕ_{bl}	sliding friction torque weighting factor (/)
ϕ_{ish}	inlet shear heating reduction factor (/)
ϕ_{rs}	kinematic replenishment/starvation reduction factor (/)
ϕ_T	thermal reduction factor (/)
κ	viscosity ratio (/)
Λ	specific film thickness (μm)
μ_{bl}	coefficient of friction in boundary film lubrication (/)
μ_{EHD}	coefficient of friction in full film lubrication (/)
μ_{sl}	sliding coefficient of friction (/)
ν	kinematic viscosity (cSt)
ν_1	required kinematic viscosity (cSt)
θ	operating temperature (°C)
θ_c	stabilization temperature (°C)
θ_s	stabilization temperature (°C)
ρ_0	density at reference temperature (g/cm^3)
ρ	density (g/cm^3)
σ	composite surface roughness roller/ring (m)
σ_1	RMS surface roughness roller (m)
σ_2	RMS surface roughness ring (m)
τ	shear stress (Pa)

References

[1] High efficiency planetary gearboxes for eco-power. World Pumps 2001;2001 (419):34-4. http://dx.doi.org/10.1016/S0262-1762(01)80327-8.

[2] E. E. Agency, Europe's onshore and offshore wind energy potential – an assessment of environmental and economic constraints, EEA Technical Report no 6; 2009, 91.

[3] Höhn B-R, Michaelis K, Vollmer T. Thermal rating of gear drives: balance between power loss and heat dissipation. AGMA Technical Paper; 1996.

[4] Martins R, Cardoso N, Seabra J. Gear power loss performance of biodegradable low-toxicity ester-based oils. Proceedings of the Institution of Mechanical Engineers Part J – Journal of Engineering Tribology 2008;222(J3):431–40, http://dx.doi.org/10.1243/13506501jet345.

[5] Martins R, Seabra J, Brito A, Seyfert C, Luther A, Igartua R. Friction coefficient in FZG gears lubricated with industrial gear oils: biodegradable ester vs. mineral oil. Tribology International 2006;39(6):512–21, http://dx.doi.org/10.1016/j.triboint.2005.03.021.

[6] Martins R, Seabra J, Seyfert C, Luther R, Igartua A, Brito A. Power loss in FZG gears lubricated with industrial gear oils: biodegradable ester vs. mineral oil. In: Dowson MPGDD, Lubrecht AA, editors. Tribology and interface engineering series, vol. 48. Elsevier; 2005. p. 421–30.

[7] Martins R, Moura P, Seabra J. Power loss in FZG gears: mineral oil vs. biodegradable ester and carburized steel vs. austempered ductile iron vs. MoS2-Ti coated steel. VDI Berichte 2005;1904.2(1904 II):1467–86.

[8] Magalhaes L, Martins R, Locateli C, Seabra J. Influence of tooth profile and oil formulation on gear power loss. Tribology International 2010;43(10):1861–71, http://dx.doi.org/10.1016/j.triboint.2009.10.001 36th Leeds-Lyon Symposium Special Issue: Multi-facets of Tribology.

[9] Eschmann P, Hasbargen L, Weigand K. Ball and roller bearings – theory, design, and application. John Wiley and Sons; 1985.

[10] SKF General Catalogue 6000 EN, SKF, November 2005.

[11] Changenet C, Velex P. A model for the prediction of churning losses in geared transmissions—preliminary results. Journal of Mechanical Design 2007;129 (1):128–33, http://dx.doi.org/10.1115/1.2403727.

[12] Changenet C, Leprince G, Ville F, Velex P. A note on flow regimes and churning loss modeling. Journal of Mechanical Design 2011;133(12):121009, http://dx.doi.org/10.1115/1.4005330.

[13] Csoban A, Kozma M. Tooth friction loss in simple planetary gears. In: Seventh international multidisciplinary conference. Baia Mare, Romania, May 17–18, 2007. p. 153-60.

[14] McNiff B, Musial W, Errichello R. Variations in gear fatigue life for different wind turbine braking strategies. In: Prepared for AWEA wind power '90, Washington, D. C. 24-8 September 1990; 1991. p. 10.

[15] Winkelmann L. Surface roughness and micropitting. In: National renewable energy laboratory wind turbine tribology seminar; 2011.

[16] McDade M. Gearbox reliability collaborative (GRC) failure database. In: National renewable energy laboratory wind turbine tribology seminar; 2011.

[17] Jungk M. Update on the development of a full life wind turbine gear box lubricating fluid. In: National renewable energy laboratory wind turbine tribology seminar; 2011.

[18] Zellmann J. Main types of damage to wind turbine gearboxes. Windkraft Journal 2009;3:2–5.

[19] Muller J, Errichello R. Oil cleanliness in wind turbine gearboxes. Machinery Lubrication; July 2002.

[20] Mitchell F. Choosing the right wind turbine lubricant. Power Engineering; April 2009.

[21] Musial W, Butterfield S, McNiff B. Improving wind turbine gearbox reliability. In: National renewable energy laboratory 2007 European wind energy conference. Milan, Italy, May 7–10, 2007. p. 13.

[22] Doll GL. Tribological challenges in wind turbine technology. In: National renewable energy laboratory wind turbine tribology seminar; 2011.

[23] Evans RD. Classic bearing damage modes. In: National renewable energy laboratory wind turbine tribology seminar; 2011.

[24] Uyama H. The mechanism of white structure flaking in rolling bearings. In: National renewable energy laboratory wind turbine tribology seminar; 2011.

[25] Cousseau T, Graça B, Campos A, Seabra J. Experimental measuring procedure for the friction torque in rolling bearings. Lubrication Science 2010;22(April 4):133–47.

[26] Fernandes CM, Martins RC, Seabra JH. Friction torque of cylindrical roller thrust bearings lubricated with wind turbine gear oils. Tribology International 2013;59:121–8.

[27] Fernandes CM, Martins RC, Seabra JH. Friction torque of thrust ball bearings lubricated with wind turbine gear oils. Tribology International 2013;58:47–54.

[28] Fernandes CM, Amaro PM, Martins RC, Seabra JH. Torque loss in cylindrical roller thrust bearings lubricated with wind turbine gear oils at constant temperature. Tribology International 2013.

[29] Hamrock BJ, Dowson D. Ball bearing lubrication. John Wiley & Sons; 1981 p. 386.

[30] Gold PW, Schmidt A, Dicke H, Loos J, Assmann C. Viscosity-pressure-temperature behavior of mineral and synthetic oils. Journal of Synthetic Lubrication 2001;18(1):51–79.